Full Paper Transactions, SMiRT 28
Toronto, Canada, August 10-15, 2025
Division V

SMATCH BENCHMARK: SEISMIC RESPONSE ANALYSES OF THE BASE-ISOLATED CRUAS NPP SUBJECTED TO THE LE-TEIL EARTHQUAKE USING THE SOFISTIK SOFTWARE

Michael Borgerhoff[1], Sara Ghadimi Khasraghy[2], Matthias Stadler[3], Tadeusz Szczesiak[4], and Rainer Zinn[5]

[1] Senior Consultant, Stangenberg & Partners Consulting Engineers, Bochum, Germany (borgerhoff@stangenberg.de)
[2] Dr., Civil Engineering Specialist, Swiss Federal Nuclear Safety Inspectorate ENSI, Brugg, Switzerland (sara.ghadimi@ensi.ch)
[3] Senior Engineer, Stangenberg & Partners Consulting Engineers, Bochum, Germany (m.stadler@stangenberg.de)
[4] Dr., Deputy Section Head, Civil Engineering Section, Swiss Federal Nuclear Safety Inspectorate ENSI, Brugg, Switzerland (tadeusz.szczesiak@ensi.ch)
[5] Dr., Senior Consultant, Stangenberg & Partners Consulting Engineers, Bochum, Germany (zinn@stangenberg.de)

ABSTRACT

In Phase 3 of the SMATCH benchmark, blind prediction and calibration calculations were carried out to assess the efficiency of engineering practices used to calculate the seismic response of the base-isolated French Cruas-Meysse NPP. An earthquake with a magnitude of 4.9 (Mw) struck Le Teil in southern France on November 11, 2019, which is approx. 15 km from the Cruas site. For the blind predictions of the seismic response, modal structural analyses were performed using the SOFiSTiK software, which were subsequently supplemented by parameter variations and a nonlinear analysis for the calibration computations. The most significant influence was exerted by variations in the modelling of the seismic isolators on which the NPP is mounted. In particular applying nonlinear material laws for the small displacements during the Le-Teil earthquake led to a good agreement with the measured data of the seismic instrumentation.

INTRODUCTION

The paper describes the numerical analyses performed in Phase 3 of the SMATCH benchmark for the French Cruas-Meysse NPP, EDF/IRSN/Egis (2023). The seismic base-isolation bearings are designed to achieve the main horizontal eigenfrequency of the isolated system of 1 Hz for the PGA level of the free-field ground motion of 0.2 g, Viallet et al. (2022). The objective of Phase 3 of the benchmark was to assess the efficiency of engineering practices for calculating the seismic response of the base-isolated Cruas NPP, performed as blind predictions in Phase 3.1 and as calibrated calculations in Phase 3.2. The analyses presented here were conducted by one of three participating teams supported by the Swiss Federal Nuclear Safety Inspectorate ENSI, using the finite element (FE) software SOFiSTiK, SOFiSTiK AG (2024). This paper presents calculated results and their comparison to the measured data in the form of acceleration response spectra and time-frequency graphs of the output signals obtained by the ENSI team Stangenberg & Partners (SPI). Furthermore, it highlights the conclusions drawn for the optimization of the calculation methods.

FINITE ELEMENT (FE) MODEL

The input geometry of the NPP was provided by the SMATCH organizers in the form of a Code_Aster software input file. A major challenge was transferring the input data to the used input language SOFiSTiK CADINP. Figure 1 shows the 3D-FE model created using the structural analysis software SOFiSTiK. The lower part of the model includes the lower and upper foundation rafts, which are connected by seismic supports consisting of elastomeric bearings placed on reinforced concrete pedestals. One of the two reactor buildings (BRI) and the auxiliary building (BAN), which house the acceleration sensors EAU_001 to EAU_003 (see Table 1), are modelled by 3D structures using shell elements. The other buildings founded on the upper foundation raft (BD1 to BD7) are represented by stick models with concentrated masses. Between lower and upper raft, 1812 elastomeric bearing elements representing the seismic isolation are situated, in groups of two, four and eight on 401 reinforced concrete pedestals. The pedestals are placed on a lower raft based on the ground. The 3D-FE model consists of approximately 115’000 shell elements, 4’500 beam elements and 1’800 spring elements.

Table 1: Positions of the EAU system sensors.

Sensor	Building	Elevation [m]
EAU_001	Reactor Building	-3.94
EAU_002	Reactor Building	+19.15
EAU_003	Auxiliary Building	-0.9

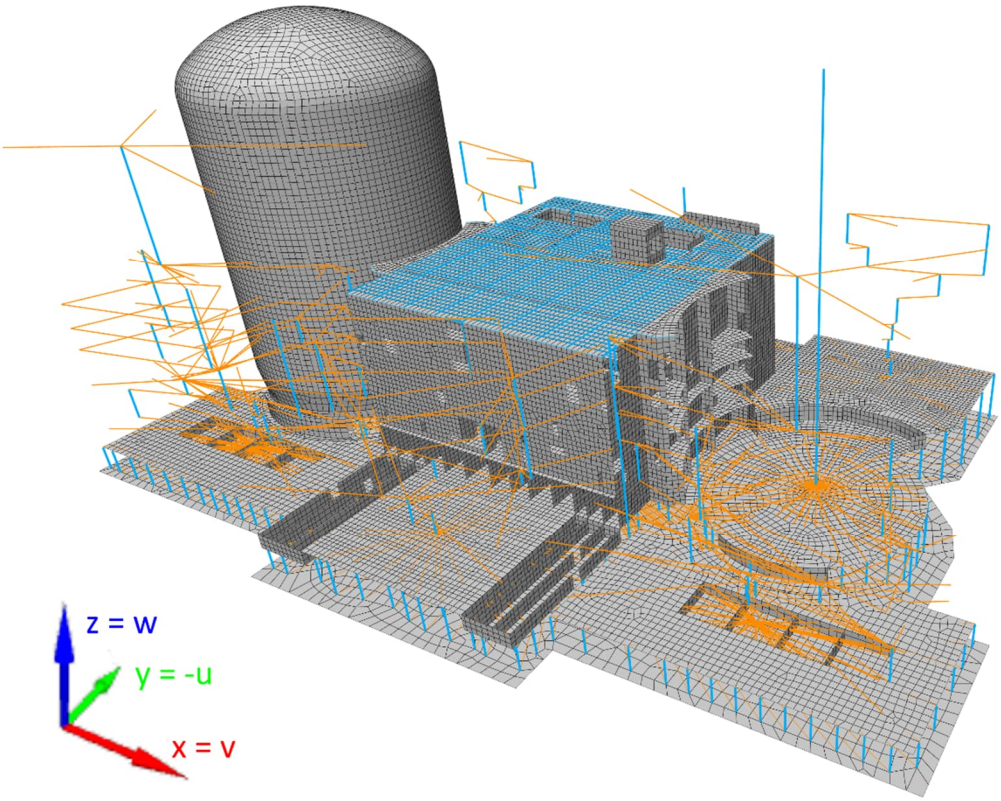

Figure 1. FE model of the Cruas NPP in SOFiSTiK.

The base isolators are simulated by three linear translational springs in the spatial directions for each seismic support. The pedestals on which the springs are located are shown in Figure 2. In the horizontal directions, the shear stiffness and in the vertical direction the compression stiffness for a single bearing pad multiplied by the number of elastomeric bearings per seismic support are assumed.

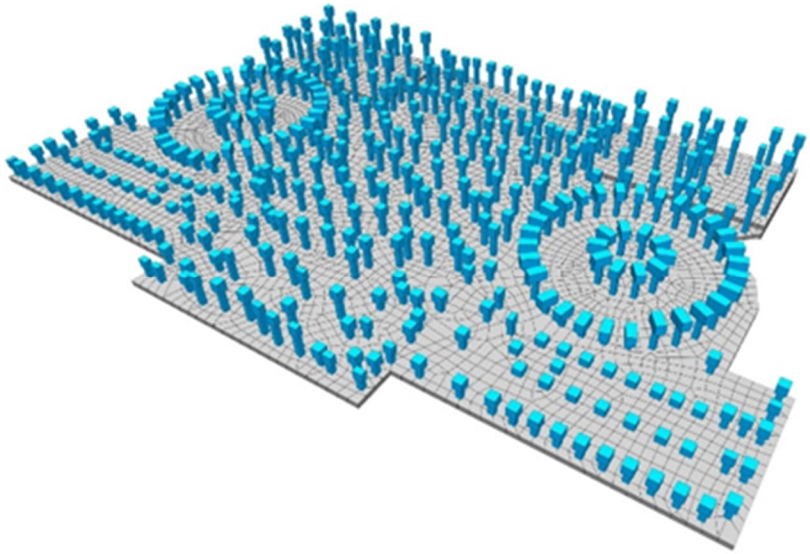

Figure 2. Detailed modelling of the seismic isolation system.

Dynamic properties of the seismic isolation

The stiffnesses of the seismic isolators assumed in Phase 3.1 were based on the shear modulus of G_d = 2.54 MPa at shear distortion γ = 0.0065 determined for the time of the Le-Teil earthquake on November 11, 2019, using age dependent dynamic properties of the seismic isolators and an aging curve of the shear modulus of the elastomeric bearings. With this shear modulus, a secant shear stiffness of K_s = 15.68 MN/m was obtained for a single bearing pad. The compression stiffness of a single bearing pad was assumed to be K_c = 5,500 MN/m. The damping ratio of the isolators was assumed to be ζ = 7% for both the horizontal and vertical directions.

Soil-structure-interaction

The soil-structure interaction (SSI) is represented by constant springs and dampers in the centre of the lower raft which is assumed as rigid. The properties of the soil springs and dampers were evaluated based on impedance functions for the level of the lower raft. The embedment was also considered in the calculation of the foundation input motion (FIM).

The analysis of the impedances and the FIM was performed using the simplified overall model of the Cruas NPP shown in Figure 3. In this model developed in SASSI software (Ostadan 2010), the upper raft is represented by a rigid support grid resting on the base isolation and the buildings are modelled by sticks with their stiffnesses adjusted to the frequencies of the individual buildings and concentrated masses at their centres of gravity.

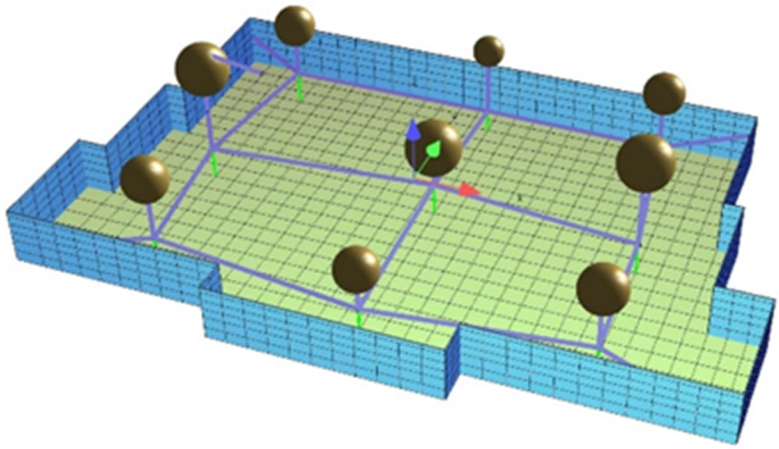

Figure 3. Simplified overall model of the Cruas NPP in SASSI.

A mean embedment depth of z = -11 m was assumed in the analysis of the impedances and the FIM. The stiffnesses and damping ratios of the six soil springs are listed in Table 2.

Table 2: Stiffnesses and damping ratios of the soil springs.

Direction	Frequency	Stiffness	Damping
X	8.3 Hz	1.451E9 kN/m	46.2 %
Y	8.3 Hz	1.712E9 kN/m	45.4 %
Z	9.8 Hz	2.180E9 kN/m	56.2 %
XX	8.3 Hz	3.630E12 kNm	14.2 %
YY	8.3 Hz	5.332E12 kNm	18.7 %
ZZ	8.3 Hz	4.090E12 kNm	28.7 %

The model shown in Figure 3 was further used for control calculations with the SSI software SASSI, for comparison with the SOFiSTiK 3D-FE model shown in Figure 1.

BLIND PREDICTIONS

In Phase 3.1 of the benchmark, blind predictions were performed using seismic excitation data provided by the SMATCH organizers from the acceleration time histories measured by the RAN sensor on the power plant site during the Le Teil earthquake. The computations were carried out as modal time history analysis with 600 eigenvalues up to a frequency of 30 Hz using a time step width of $\Delta t = 0.005$ s. The important fundamental frequencies calculated in the blind predictions are $f_7/f_8/f_9 = 1.33/1.36/1.38$ Hz in the horizontal directions and $f_{75} = 8.75$ Hz in vertical direction. The modal masses achieved at 30 Hz are more than 98% in all spatial directions.

The comparison of the acceleration response spectra calculated in Phase 3.1 with the response spectra resulting from the acceleration time histories measured with the EAU seismic instrumentation is

shown in Figure 4. It is primarily evident that the spectral peaks at the fundamental frequencies caused by the seismic isolation differ from each other in terms of both frequencies and amplitudes, see, for example, spectra at the EAU_002 sensor at elevation +19.15 m in the reactor building BRI. The calculated eigenfrequencies of the seismically isolated structure are approximately 14% smaller than those derived from the measurements.

Another significant deviation between the calculated and the measured response spectra were the higher measured horizontal accelerations in the frequency range above 4 Hz, particularly measured at the EAU_002 sensor, which were not reproduced by the computations in Phase 3.1.

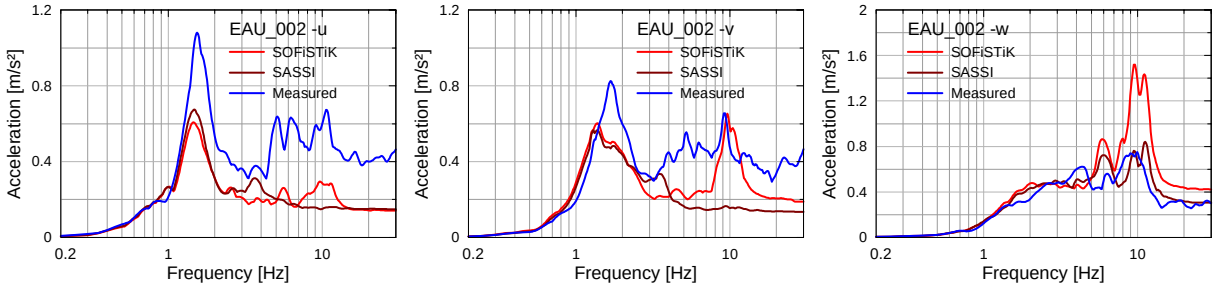

Figure 4. Blind prediction, response spectra D = 5% at the EAU_002 sensor location.

CALIBRATION COMPUTATIONS

In Phase 3.2, the calculated eigenfrequencies and response spectra were compared with the measured values of the seismic instrumentations and the computational parameters were calibrated accordingly. As part of the calibration, various parametric studies were carried out and the resulting effects were evaluated. The changes to the final calculation models between Phase 3.1 and Phase 3.2 are listed below.

1) As part of the calibration of the calculation model in Stage 3.2 based on the acceleration measurements, the following adjustments were made to the assumptions regarding the horizontal stiffness of the seismic isolators:

- Direction u (increase by factor 1.4): G_d = 3.56 MPa, K_s = 21.95 MN/m
- Direction v (increase by factor 1.7): G_d = 4.32 MPa, K_s = 26.66 MN/m

This increased the calculated fundamental frequencies from $f_7/f_8/f_9$ = 1.33/1.36/1.38 Hz to $f_7/f_8/f_9$ = 1.55/1.59/1.66 Hz. Calculated amplitudes of the spectral peaks also increased which led to a good agreement with the measured values.

2) The blind prediction revealed an inexplicable resonance frequency of close to 10 Hz in the x (v) and z (w) directions for the EAU_002 sensor, see Figure 4. This resonance was caused by a vertical eigenmode of the internal structure of the reactor building, which in turn caused a horizontal vibration in the x-direction at the height of the EAU_002 sensor. When checking this oscillation, it was observed that the walls of the biological shield in the model were not connected to the upper raft. Instead, there was a distance of 0.29 m between the lower end of these walls and the -3.5 m level without any connections. In the model, the biological shield was therefore only supported by the surrounding ceilings. Closing the gap between the biological shield and the upper raft by couplings influenced the response spectra at the EAU_002 sensor in v- and w-direction in such a way that the spectral peak between 9 and 10 Hz disappeared in v-direction and became significantly smaller in w-direction.

3) The damping ratio of the isolators in the vertical direction was changed from ζ = 7% to ζ = 2%. This change had no influence on the response spectra.

4) The damping value assumed in Phase 3.1 to be ζ = 2% for the reinforced concrete structure was reduced to ζ = 1% due to the comparatively low seismic load. This change led to an increase in the spectral accelerations, especially in the horizontal directions above 4 Hz. The spectral peak at 1.6 Hz was not affected.

5) The incoherence of the earthquake excitation according to the Abrahamson soil model was considered. The computation was conducted using the SASSI model shown in Figure 3. The incoherence of the earthquake excitation only affected the vertical accelerations of higher frequencies > 6 Hz, which was decreased by approximately 15%. This parameter is considered in the resulting vertical spectra.

With these adjustments, the calibration achieved a good agreement between calculated and measured spectral accelerations – apart from some remaining deviations for accelerations in the frequency range above 4 Hz. The response spectra for the three sensors of the EAU system resulting from the best-estimate computation Run 07 in u, v, and w directions are shown in Figure 5, Figure 6 and Figure 7.

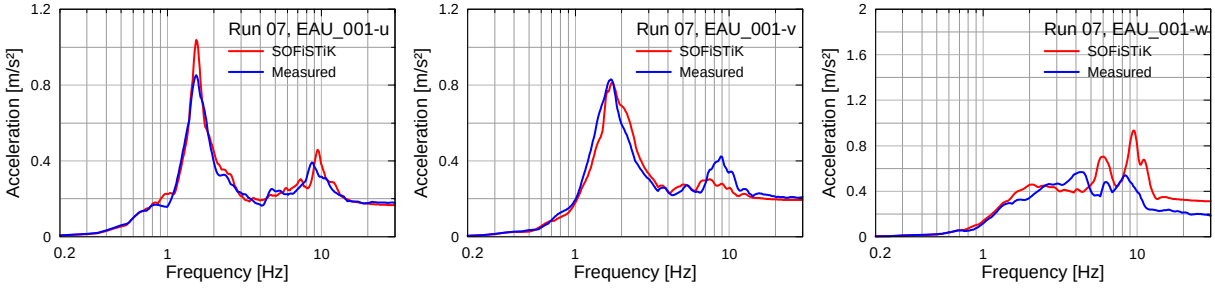

Figure 5. Best-estimate computation, response spectra D = 5% at the EAU_001 sensor location.

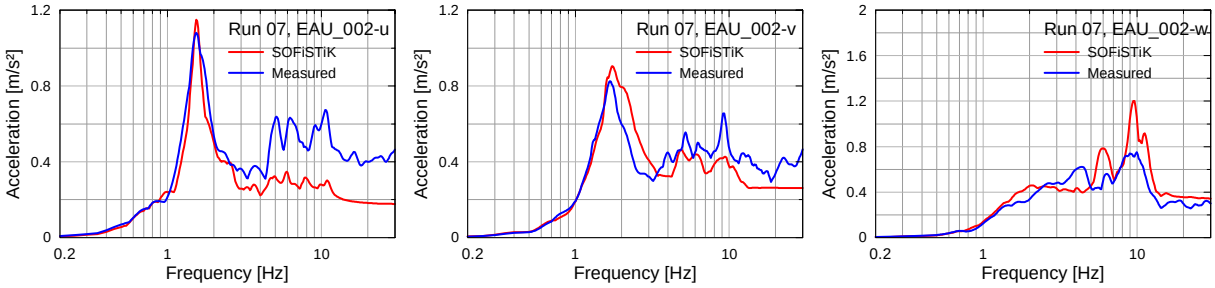

Figure 6. Best-estimate computation, response spectra D = 5% at the EAU_002 sensor location.

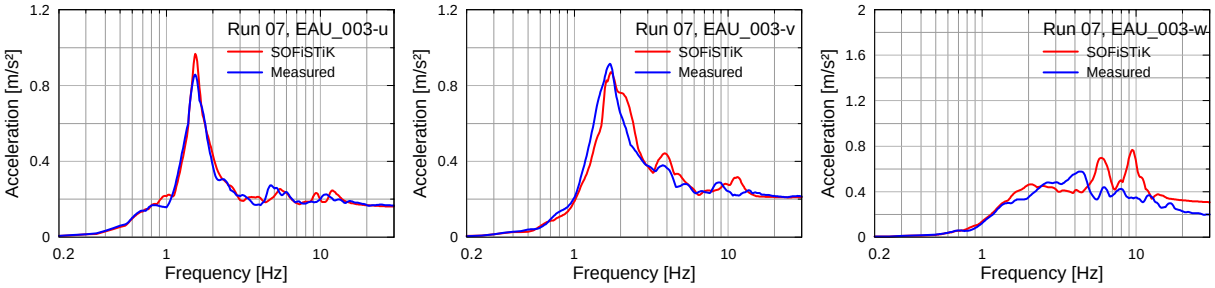

Figure 7. Best-estimate computation, response spectra D = 5% at the EAU_003 sensor location.

The time-frequency graphs of the output signals requested in the benchmark to analyse the frequency content of the acceleration-time histories were determined using continuous wavelet transforms (CWT). Figure 8 shows an example of the time-frequency- graphs (Stockwell Transform) of the EAU_002 sensor in the three spatial directions. In the graphs of the horizontal directions u and v, the frequency band caused by the fundamental eigenfrequencies is clearly visible at about 1.5 Hz. In the graph of the unfiltered vertical direction w, other structural eigenfrequencies are significant.

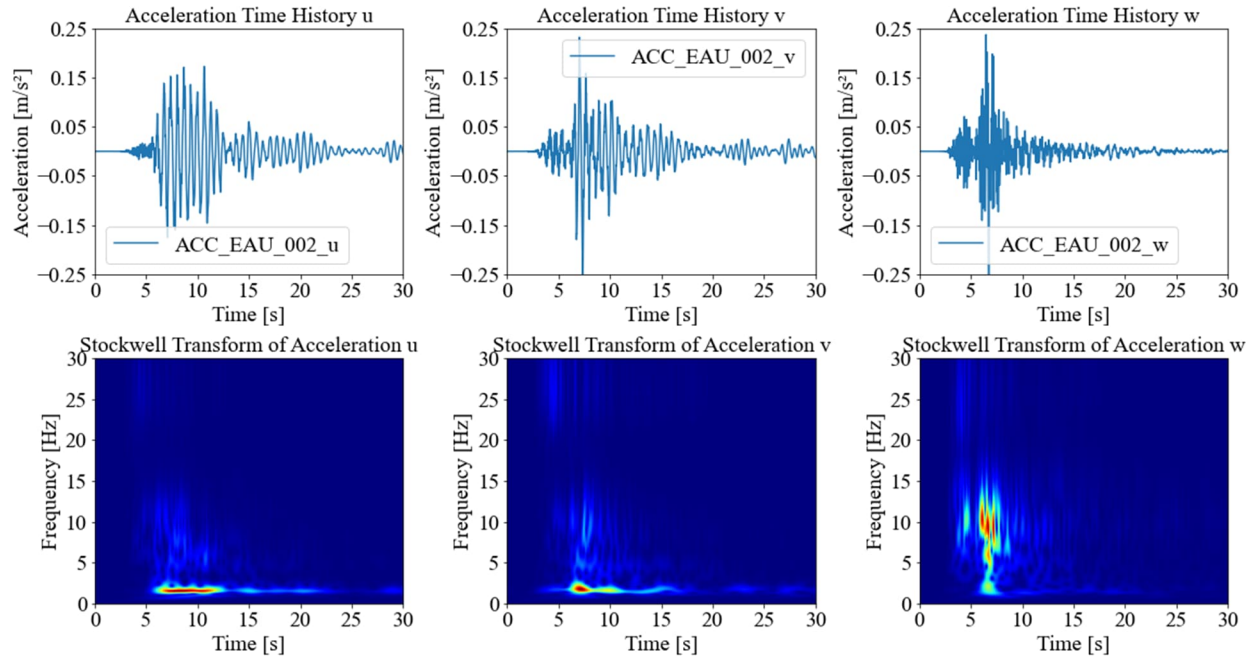

Figure 8. Time-frequency graphs of acceleration-time histories of sensor EAU_002, determined using continuous wavelet transform (CWT).

STUDY INCLUDING NONLINEAR BEHAVIOUR OF ELASTOMERIC BEARINGS

There were horizontal accelerations measured above 4 Hz, especially at the EAU_002 sensor (see Figure 4), which were not reproduced in the blind and calibration calculations. The objective of the study carried out in addition to the calibration computations, was to investigate how considering the nonlinear behaviour of the elastomer bearings affects the calculated accelerations in the frequency range above 4 Hz.

The study includes calculations with two nonlinear force-displacement laws for the elastomeric bearings. These are based on the grid points specified in Table 3 for the logarithmic approximation of the nonlinear relationship of the dynamic shear modulus G_d as a function of the shear distortion γ:

$$G_d = c_1 \cdot \ln(\gamma) + c_2 \quad (1)$$

The linear stiffness of one bearing k = 15.68 MN/m is based on G_d = 2.54 MPa, which was derived for the Le-Teil earthquake distortion γ = 0.0065 from the progressive distortion test data in Phase 3.1.

Table 3: Grid points of nonlinear force-displacement laws.

	Point 1	Point 2
Work Law 1	k = 15.68 MN/m x 1.55 at u = 1.0 mm	G_d = 2.54 MPa at γ = 0.0065
Work Law 2	k = 15.68 MN/m x 1.7 at u = 0.5 mm	G_d = 2.54 MPa at γ = 0.0065

The two resulting work laws WL1 and WL2 are shown in Figure 9 in comparison to the linear stiffness k = 15.68 MN/m assumed in Stage 3.1. The course of the curves beyond the displacement of 2.6 mm at γ = 0.0065 are irrelevant for the present investigation, since this displacement range is not reached.

The force-displacement laws shown in Figure 9 correspond to a single bearing and are multiplied in the calculation by a factor corresponding to the number of bearings per pedestal (2, 4 or 8). The increases in horizontal stiffness of the seismic isolation applied in Phase 3.2 are thus now implicitly included for small displacements.

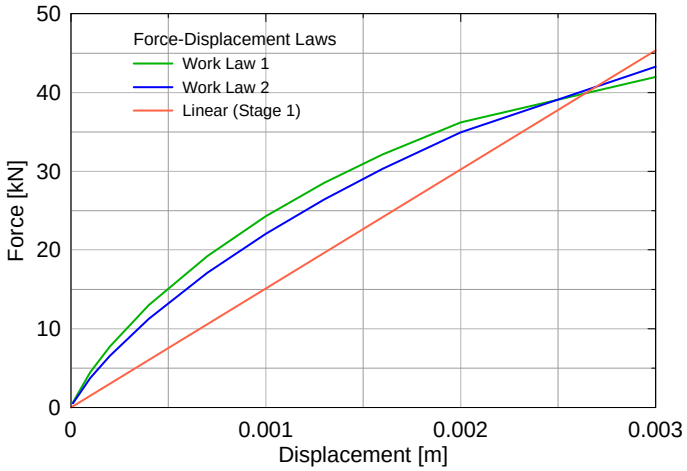

Figure 9. Force-displacement laws for a single bearing.

The nonlinear force-displacement behaviour of the elastomeric bearings is represented by a hyperelastic material behaviour (material model HYPE in SOFiSTiK). Since this model does not imply hysteretic damping, a predefined damping of ζ = 7% is introduced.

The horizontal displacements of the nonlinear computation with work law 1 in comparison with the linear computation Run07 (best-estimate computation) is depicted in Figure 10 for the sensor EAU_001.

The maximum displacements remain below 2 mm. A maximum displacement of 2.6 mm is documented in EDF/IRSN/Egis (2023) but without mentioning place and direction of this measured displacement.

The response spectra at the location of EAU_002 sensor according to Figure 11 show that the accelerations calculated with nonlinear spring characteristics in the frequency range above 4 Hz are larger than those calculated linearly and better match the measured values. A possible reason for this interesting effect could be that for very low displacements the stiffness of the isolators is high.

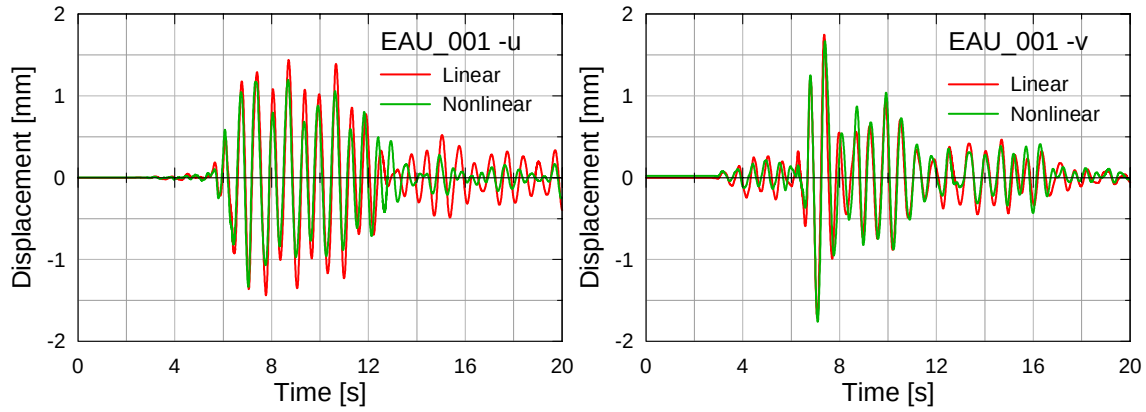

Figure 10. EAU_001, displacements obtained by linear and nonlinear modelling of isolators.

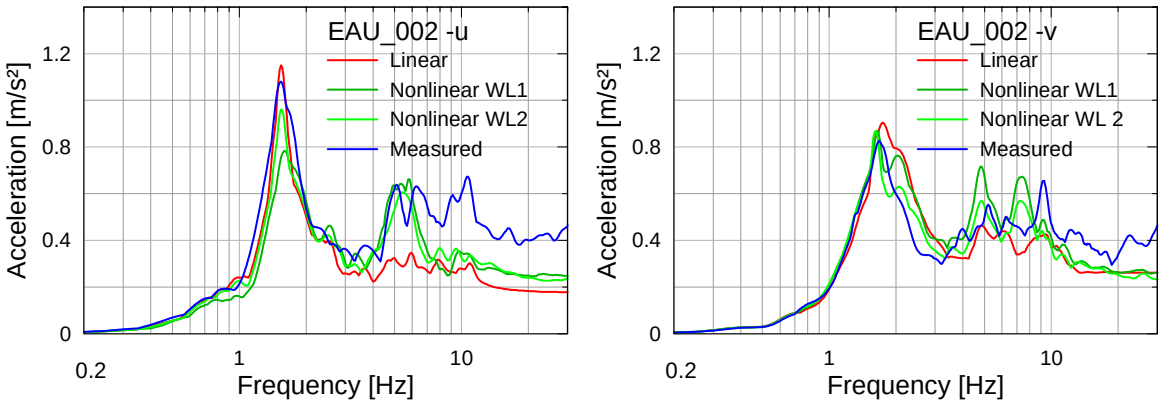

Figure 11. Comparison of response spectra D = 5% at the EAU_002 sensor obtained by linear and nonlinear modelling of isolators.

CONCLUSIONS

Numerical analyses were performed as part of the SMATCH benchmark for the French Cruas-Meysse NPP to assess the efficiency of engineering practices of calculating the seismic response of the base-isolated NPP. The blind predictions for Phase 3.1 of the benchmark were conducted as modal time history analyses using a FE model of the NPP provided by the SMATCH organizers, which was transferred to the used FE software SOFiSTiK. The comparison of the results of the blind predictions with the measured data showed deviations of about 14 % for the main frequencies. Additionally, some higher measured accelerations in the range above 4 Hz could not be reproduced by the linear computations. Therefore, calibration calculations were carried out in Phase 3.2, in which isolator stiffnesses and damping values were adjusted. Furthermore,

an additional study was conducted using nonlinear representation of the isolators. With these changes, a good agreement with the measured data was achieved. The specific peaks in the higher frequency range of the response spectra could only be captured using a nonlinear material law for the isolators.

The degree of realism of FE-based computations could be significantly increased by benchmarking against real measurements and subsequent calibration and by identifying the causes of deviations between the numerical model and the real structural response.

This study also shows that for a base isolated structure the properties of the bearings must correspond to the expected stress and displacement level for a realistic seismic analysis.

REFERENCES

EDF/IRSN/Egis (2023): SMATCH Benchmark, Seismic Base Isolated Nuclear Power Plant Shaken by a Real Earthquake, https://smatch-benchmark.org/.

Ostadan, F. (2010): SASSI 2010, A System for Analysis of Soil-Structure Interaction, Version 1.0.

SOFiSTiK AG (2024): SOFiSTiK Analysis Programs, Version 2024-9 Build 1091, Oberschleißheim, Germany.

Viallet, E., Berger, J., Traversa, P., El Haber, E., Hervé-Secourgeon, E., Hervé-Secourgeon, G., Zuchowski, L., Dupuy, G. (2022). “2019-11-11 Le Teil Earthquake – The Ultimate Missing Piece of Experience Feedback Related to a Nuclear Power Plant Built on Seismic Base Isolation: A Real Earthquake”, Transactions of the SMiRT 26, Potsdam, Germany.